

Atomic scattering from Bose-Einstein condensates

Ivo Häring and Jan-Michael Rost

Max-Planck-Institute for the Physics of Complex Systems, Nöthnitzer Str. 38,
D-01187 Dresden, Germany

Abstract. Elastic scattering probes directly the interaction potential. For weakly interacting condensates this potential is given by the condensate density. We investigate how the differential and total cross sections reflect the density. In particular, we have determined which signatures the Thomas Fermi approximation leaves in contrast to an exact solution for the condensate wave function within the Gross-Pitaevskii theory.

After the pioneering experimental realization of Bose-Einstein condensation in magnetically trapped atomic gases [1, 2, 3] these condensates are now routinely generated in many laboratories around the world. Consequently the interest is shifting from the production and structure of the condensates to their dynamics, i.e., their interaction with matter and radiation. One fundamental form of interaction is scattering. While it is not entirely clear up to now (see, e.g., [4]) how to perform experimentally a "standard" scattering experiment (that is to generate projectiles with the appropriate extremely low absolute kinetic energies) first theoretical studies have explored possible effects [5].

The purpose of our work is to investigate the signatures of the target distribution (i.e. the spatial condensate density) in the elastic cross section. In particular, we are interested in the differences between an exact description of the density in the framework of the Gross-Pitaevskii theory and the additional Thomas Fermi approximation which allows one to determine the condensate density analytically in the limit of a dense and strongly repulsive atomic gas.

We will study these effects in the first Born approximation (see also [5]) a natural starting point for collisionally probing a system at high impact energies (in terms of the binding energy of the target, i.e. the condensate). We start from the same setup for the weakly coupled many-body Bose system as in [4] and decompose the Hamiltonian from the beginning into

$$H = H_T + H_P + U \quad (1)$$

where H_T stands for the target part containing the condensate, H_P represents the projectile Hamiltonian of the impinging atom and U describes its interaction with the target atoms. The target Hamiltonian reads

$$H_T = \int d^3r \hat{\Psi}^\dagger(\mathbf{r}) \left(-\frac{\hbar^2}{2m} \Delta_{\mathbf{r}} + V_{\text{ex}} + V_a(\mathbf{r}) \right) \hat{\Psi}(\mathbf{r}), \quad (2)$$

where $\hat{\Psi}(r)$ is the field operator for destruction of bosons at \mathbf{r} , $V_{\text{ex}} = m\omega^2 r^2/2$ is the harmonic trapping potential. The contact interaction between the atoms of mass m is expressed through the s-wave scattering length a_s as

$$V_a(\mathbf{r}) = \frac{1}{2} \int d^3r' \hat{\Psi}^\dagger(\mathbf{r}') V(\mathbf{r}, \mathbf{r}') \hat{\Psi}(\mathbf{r}') \quad (3)$$

with

$$V(\mathbf{r}, \mathbf{r}') = 4\pi\hbar^2 a_s/m \delta(\mathbf{r} - \mathbf{r}'). \quad (4)$$

For simplicity we consider projectile atoms of the same sort as the condensate atoms. Hence, the interaction potential

$$U(\mathbf{r}_p) = 2V_a(\mathbf{r}_p) \quad (5)$$

of the condensed atoms with the projectile atom is of the same form as the potential $V_a(\mathbf{r})$ within the condensate, given in (3), where \mathbf{r}_p is the position of the projectile atom. The factor two has its origin in the single particle nature of the interaction of the scattering atom with the condensed atoms.

In the weak coupling limit we may write the field operator as [6]

$$\hat{\Psi}(\mathbf{r}) = N_0^{1/2}\Psi_0(\mathbf{r}) + \delta\hat{\Psi}(\mathbf{r}) \quad (6)$$

where Ψ_0 is a c-number whose squared modulus represents the normalized density of the condensate at position \mathbf{r} . Minimizing the grand canonical Hamiltonian $K_T = H_T - \mu N_T$, where N_T is the number operator of the trapped atoms, with respect to the functional $[\Psi_0]$ to zeroth order in $\delta\hat{\Psi}(\mathbf{r})$ gives the time-independent Gross-Pitaevskii equation for the condensate wave function Ψ_0

$$\left(-\frac{\hbar^2}{2m}\Delta_{\mathbf{r}} + V_{\text{ex}} + N_0 4\pi\hbar^2 a_s/m |\Psi_0|^2 - \mu \right) \Psi_0 = 0. \quad (7)$$

The eigenvalue μ is the chemical potential. With (6) and Ψ_0 from (7) one obtains the elementary quasiparticle excitation modes and energies by diagonalizing K_T to second order in $\delta\hat{\Psi}$. This is the ‘‘standard’’ Bogolubov approximation [7, 8].

However, in the present context we are only interested in elastic collisions. In leading order of the number of condensed atoms N_0 the excitations do not contribute to these processes as we will see shortly.

The asymptotic scattering states are eigenstates of H_T and H_P respectively, i.e. condensate eigenstates $|\Phi_i\rangle$ and $|\Phi_f\rangle$ as described above, and plane waves for the projectile atom with asymptotic initial and final momenta \mathbf{k}_i and \mathbf{k}_f , respectively. With equation (5) the scattering amplitude in first Born approximation reads then

$$F(\theta, \phi) = -\frac{m}{2\pi\hbar^2} \int d^3r e^{-i\mathbf{k}_f \mathbf{r}} \langle \Phi_f | U(\mathbf{r}) | \Phi_i \rangle e^{i\mathbf{k}_i \mathbf{r}} \quad (8)$$

with the cross section defined as

$$\frac{d\sigma}{d\Omega} = \frac{k_f}{k_i} |F(\theta, \phi)|^2. \quad (9)$$

Inserting (6) into (8) and keeping only leading terms in N_0 one obtains the elastic scattering amplitude

$$F_{\text{el}}(\theta, \phi) = -2a_s \int d^3r e^{-i\mathbf{q}\mathbf{r}} N_0 |\Psi_0(\mathbf{r})|^2 \quad (10)$$

where $\mathbf{q} = \mathbf{k}_f - \mathbf{k}_i$ is the vector of momentum transfer and no energy has been exchanged between initial and final state, i.e. $\Phi_i = \Phi_f$ and $|\mathbf{k}_i| = |\mathbf{k}_f| \equiv k$.

From (10) one can see that the elastic cross section probes directly the condensate density $|\Psi_0|^2$. For structural properties of repulsive atomic gases with large particle number N_0 it is often sufficient to determine Ψ_0 in the Thomas-Fermi approximation [9] as applied, e.g., in [5].

Its justification is most easily seen if one scales the unit length and energy in (7) such that the only remaining parameter appears as an effective mass Γ . Before doing so, we separate the relevant radial s-wave part by the substitution $\Psi_0(r) = u(r)/r(4\pi)^{-1/2}$ and obtain in energy and length units of the trapping potential, namely $\hbar\omega$ and $a_\omega = [\hbar/(m\omega)]^{1/2}$,

$$\left(-\frac{1}{2}\frac{d^2}{dr^2} + \frac{r^2}{2} + \Gamma\frac{u(r)^2}{r^2} - \frac{\mu}{\hbar\omega}\right)u(r) = 0 \quad (11)$$

where

$$\Gamma = N_0 a_s / a_\omega. \quad (12)$$

Scaling the length in (11) according to $r = \Gamma^{1/4}x$, dividing (11) by $\Gamma^{1/2}$, and defining $\bar{u}(x) = u(r)$ leads to

$$\left(-\frac{1}{2\Gamma}\frac{d^2}{dx^2} + \frac{x^2}{2} + \frac{\bar{u}(x)^2}{x^2} - \bar{\mu}\right)\bar{u}(x) = 0, \quad (13)$$

where $\bar{\mu} = \mu/\hbar\omega\Gamma^{1/2}$. For large Γ the kinetic energy becomes small and is neglected in the Thomas Fermi approximation (TFA). This leads to the solution

$$u(r)/r = (\mu/\Gamma(1 - (r/R)^2))^{1/2}, \quad (14)$$

where $\mu(\Gamma) = \hbar\omega/2(15\Gamma)^{2/5}$ is obtained from the normalization condition $\int u^2(r)dr = 1$. It defines simultaneously the cutoff $R(\Gamma) = a_\omega(15\Gamma)^{1/5}$ which obeys the relation

$$\mu = \frac{m\omega^2}{2}R^2. \quad (15)$$

The solution of (11) must be obtained numerically, e.g., by imaginary time propagation with the Split Operator Method [10].

From the construction it is clear that the TFA is only applicable for large and positive Γ which implies according to (12) a positive scattering length $a_s > 0$ and under realistic experimental conditions a large particle number $N_0 \gg 1$. This is illustrated in figure 1 where the (normalized) solution $\Psi_0(r)$ of (7) is compared to the TF-approximate solution (14). Significant differences appear for $\Gamma < 10$, for the order parameter (part a) as well as for the chemical potential (part b). However, from problems involving a simple atom as a target, one knows that elastic scattering at higher impact energies probes the target distribution to some detail. Hence, it is a priori not clear to what extent the TFA describes cross sections well, even in a parameter regime for $\Gamma \gg 1$ where it works well for structural properties. For total elastic cross sections the best agreement, as expected, is obtained at low impact momentum k (figure 2). The functional dependence on k is the same for the exact solution and the TFA approximation for large k and can be derived from the TFA approximation to be $\sigma(kR \gg 1) \propto (Rk)^{-2}$, where $R = a_\omega(15\Gamma)^{1/5}$ is the condensate radius in the TFA approximation, see (14). However, the exact solution and the TFA differ by a factor which grows with decreasing Γ (figure 3a).

On the other hand, the total cross section for the TFA in the Born approximation can be mapped to a single universal curve if one scales $\tilde{\sigma} = \sigma/\Gamma^2$ and expresses the momentum in the dimensionless variable $\tilde{k} = kR$ where R is the cutoff parameter of (15). The numerical solution does not have a well defined cutoff parameter (see figure 1a). However, we may use (15) to define the cutoff R_μ from the numerically obtained chemical potential μ . With this scaling the cross sections from the numerical order parameter fall onto the same universal curve as the TF cross sections (3b).

Considerably more disagreement between the TFA and the exact solution is seen in the differential cross section shown as a function of momentum transfer in figure 4. One clearly recognizes the exponential versus the algebraic decrease in the absolute magnitude and the different oscillatory behavior. Both effects can be understood analytically. The "soft edge" of the numerically obtained condensate distribution leads to an exponential decrease of the cross section with increasing q . A similar effect occurs in the photoionization and the Born cross section for scattering of metal (jellium) clusters due to a soft edge in the electron distribution [11, 12]. On the other hand, the "hard edge" of the analytical TFA distribution (14) produces via Fourier transform the (unphysical) algebraic decrease of the differential cross section. (In the photoionization of clusters this would correspond to a box-like electron distribution with a sharp cut-off, [11]). For the oscillatory behavior we note that the exact cross section oscillates asymptotically for large q and Γ with the same frequency as the TF approximated cross section given by the condensate radius R .

Overall we conclude that the TFA offers also for scattering problems a reasonably good approximation as long as Γ is not too small. Significant deviations from the exact solution occur only for large momentum transfer q for which the cross sections are so small that they will not be experimentally accessible.

References

- [1] Anderson M H, Ensher J R, Matthews M R, Wieman C E and Cornell E A 1995 *Science* **269** 198
- [2] Davis K B, Mewes M-O, Andrews M R, van Druten N J, Durfee D S, Kurn D M and Ketterle W 1995 *Phys. Rev. Lett.* **75** 3969
- [3] Bradley C C, Sackett C A, Tollett J J and Hulet R G 1995 *Phys. Rev. Lett.* **75** 1687
- [4] Wynveen A, Setty A, Howard A, Halley J W and Campell C E 2000 *Phys. Rev. A* **62** 023602
- [5] Idziaszek Z, Rzążewski K and Wilkens M 1999 *J. Phys. B* **32** L205
- [6] Bogolubov N 1947 *J. Phys. (USSR)* **11** 23
- [7] Fetter A F 1972 *Ann. Phys. (NY)* **70** 67
- [8] Griffin A 1996 *Phys. Rev. B* **53** 9341
- [9] Goldman V F and Silvera I F 1981 *Phys. Rev. B* **24** 2870
- [10] Fleck J A, Morris J R, and Feit M D 1976 *Appl. Phys.* **10** 129
- [11] Frank O and Rost J M 1996 *Z. Phys. D* **38** 59
- [12] Keller S, Engel E, Ast H and Dreizler R M 1997 *J. Phys. B* **30** L703

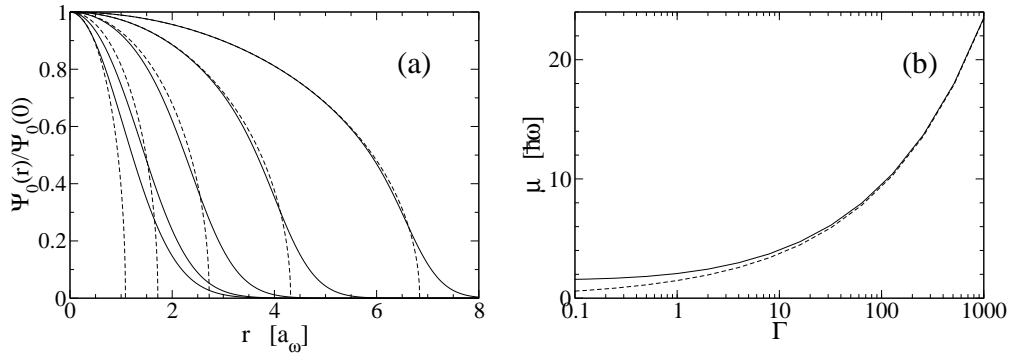


Figure 1. Properties of the numerical (*solid*, (11)) and Thomas Fermi (*dashed*, (14)) solution of the Gross-Pitaevskii equation. Part (a) presents the order parameter $\psi_0(r)$ normalized to unity at $r = 0$ for $\Gamma = 1/10, 1, 10, 100, 1000$ (from left to right). Part (b) shows the chemical potential as a function of Γ .

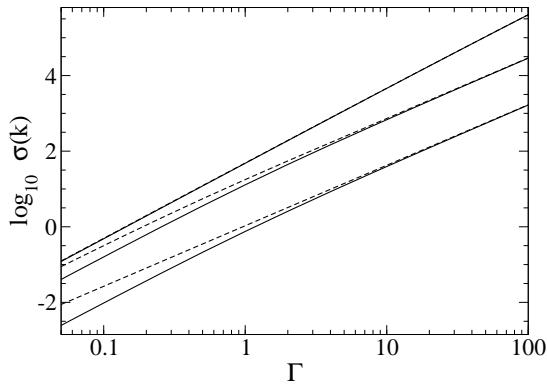


Figure 2. Total elastic cross sections as a function of Γ for $k = 0.2, 1.2, 5$ from top to bottom. Coding of the lines as in figure 1.

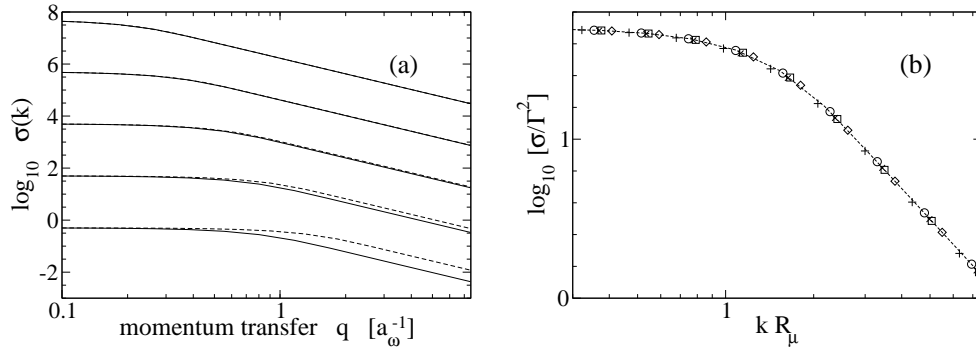


Figure 3. (a) Total elastic cross sections for the same Γ values as in figure 1a from top to bottom. Part (b) shows the cross sections of (a) in scaled coordinates, see text. The symbols (+, \times , \circ , \square , \diamond) correspond to $\Gamma = 1/10, 1, 10, 100, 1000$ and the dashed line is the universal TF curve.

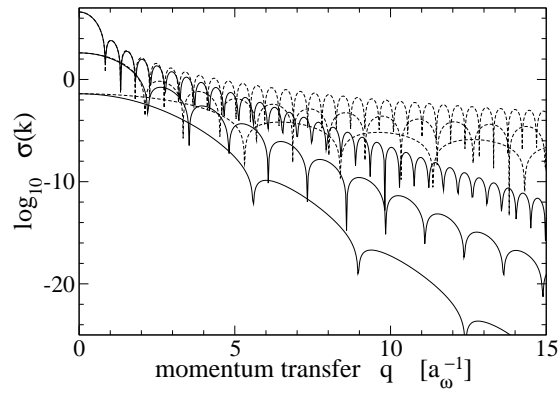


Figure 4. Differential elastic cross sections as a function of momentum transfer q for $\Gamma = 1/10, 10, 1000$ from bottom to top in both the group of numerical cross sections (*solid*) and analytical cross sections (*dashed*).